2026 JULY 19–22 VANCOUVER, BC
JOINT AAPM | COMP MEETING

Effects on Tumor Metabolism in Repetitive MRI Measurements Using Hyperpolarized Pyruvate

Qing Wang, PhD[1]; Yunyun Chen, PhD[2]; Vencel Somai, PhD[3]; Galen Reed, PhD[3]; Collin Harlan[1,4]; Ryan Boyce[1]; Myriam Chaumeil, PhD[3]; Stephen Y. Lai, MD, PhD[2], James Bankson, PhD[1,4]

[1]Department of Imaging Physics, Division of Diagnostic Imaging, The University of Texas MD Anderson Cancer Center, Houston, TX, United States,
[2]Department of Head and Neck Surgery, Division of Surgery, The University of Texas MD Anderson Cancer Center, Houston, TX, United States,
[3]NVision Imaging Technologies GmbH, Ulm, Germany,
[4]The University of Texas MD Anderson Cancer Center UTHealth Graduate School of Biomedical Sciences, Houston, TX, United States

ABSTRACT

Purpose: To investigate the dependence of tumor metabolism on hyperpolarized (HP) pyruvate concentration, administration order, and time interval in repeated MRI measurements.

Methods: Ten anaplastic thyroid cancer (ATC) tumor-bearing mice (Hth83 cells) were imaged under IACUC-approved protocols. Three mice received 40mM HP pyruvate administered first followed by 80mM after 0.5-hour interval (Polaris polarized) within the same imaging session. Four mice received 40mM first followed by 80mM after 24 hours (Hypersense polarized). Three mice received 80mM first followed by 40mM after 24 hours (Hypersense polarized). MRI experiments were performed on a 7T Biospec Bruker system[5]. Image reconstruction and data analysis were performed in MATLAB R2024b (MathWorks, Natick, MA).

Results: ATC mice tumor tissue exhibited consistent metabolic tendency between two pyruvate concentrations. Across ten paired measurements, higher k_{PL} values were observed following the 40mM HP pyruvate injection than 80mM injection when tumor metabolism was quantified using the area under the curve (AUC) and precursor-product k_{PL} (Wilcoxon signed-rank test, $p < 0.05$). When scanning conditions varied (0.5-hour interval, 24-hour interval and 24-hour interval with reverse injection order), similar metabolism trend can be observed when using precursor-product k_{PL}.

Conclusions: We investigated tumor-region metabolism in ATC mice following successive HP pyruvate injections with varying concentration, administration order, and time interval. Different metabolism quantification approaches were used. Our results show that metabolism was consistently higher for the 40mM injection than for the 80mM injection and was robust to injection order and time interval when using AUC ratio and precursor-product k_{PL}. This indicated that consecutive HP pyruvate injections provide reproducible metabolic measurements in repetitive studies.

CONTACT

[Qing Wang]
[UT MD Anderson Cancer Center]
[Houston]
[qwang18@mdanderson.org]

INTRODUCTION

Hyperpolarized (HP) ^{13}C pyruvate MRI provides a powerful approach for noninvasively assessing tumor metabolism by quantifying the pyruvate-to-lactate conversion rate constant, k_{PL}[1-3]. However, the factors influencing k_{PL} variation between repeated HP pyruvate measurements remain incompletely understood. Therefore, this study investigated tumor-region k_{PL} using consecutive HP pyruvate injections with varying concentrations, time intervals, and administration orders in anaplastic thyroid cancer (ATC) mice model. Multiple metabolic quantification approaches were applied to evaluate the robustness and reproducibility of tumor metabolic measurements under different injection conditions.

METHODS AND MATERIALS

Material: Aliquots of ^{13}C pyruvic acid were polarized using Polaris (NVision Imaging Technologies) or HyperSense (Oxford Instruments). Following dissolution, two HP pyruvate solutions were prepared: 40mM (diluted with saline) and 80mM (undiluted), and 200µL of each was administered via tail-vein catheter accordingly.
Modelling: ATC mice tumor tissue metabolism was quantified using following approaches: HP pyruvate to lactate area under the curve (AUC) ratio; precursor-product pyruvate to lactate conversion rate, k_{PL}; two-compartment two-chemical pools pharmacokinetic (PK) model k_{PL} and simplified three compartment PK model k_{PL}[4].
Statistical analysis: Willcoxon signed-rank test was used to evaluate metabolic differences between the 40mM and 80mM pyruvate injection groups.

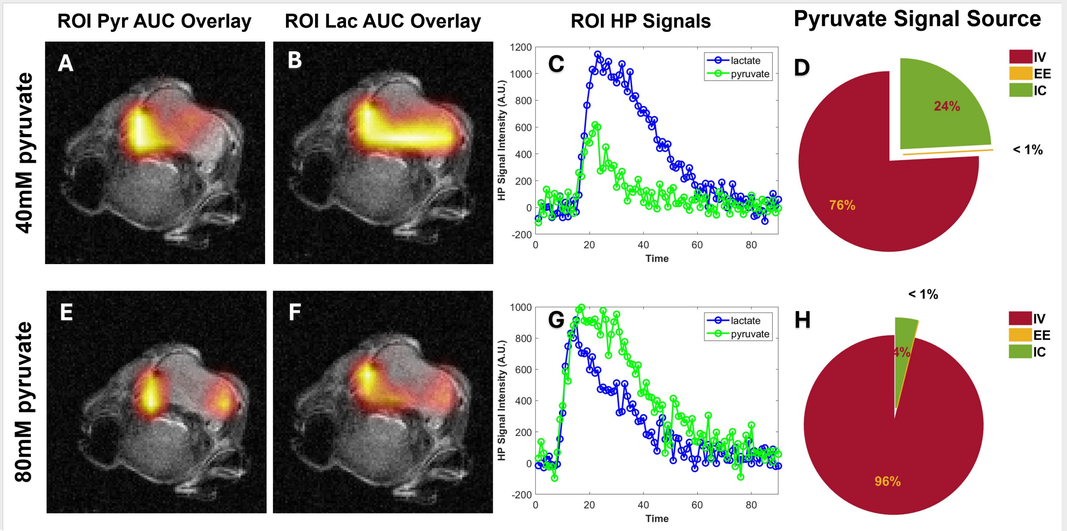

Figure 1. (**A**, **B**) Representative HP ^{13}C pyruvate and lactate maps acquired from a thyroid tumor-bearing mouse following a 40mM HP pyruvate injection. **(C)** Dynamic HP pyruvate and lactate signals extracted from the tumor region of interest (ROI). **(D)** Pyruvate fractions estimated using a simplified 3-compartment 2-chemical-pool pharmacokinetic (PK) model based on the dynamic HP signals shown in **C**. (**E, F**) Representative HP ^{13}C pyruvate and lactate maps acquired from the same mouse following an 80mM HP pyruvate injection 24 hours later. **(G)** Dynamic HP signals from the tumor ROI. **(H)** Model-derived pyruvate fractions based on the dynamic HP signals shown in **G**.

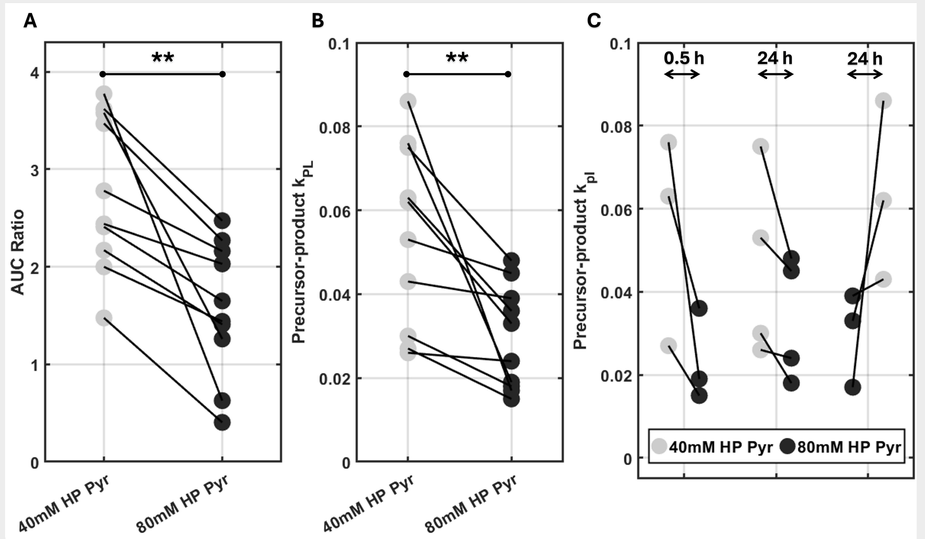

Figure 2. **(A)** Tumor metabolism in ATC mice quantified using HP pyruvate to lactate AUC ratio. Metabolic measurements following the 40mM and 80mM HP pyruvate injections are compared, with a significant difference observed between the two groups (N = 10, p value = 0.002). **(B)** Tumor metabolism quantified using the precursor-product k_{PL}. The fitted k_{PL} differed significantly between the 40mM and 80mM HP pyruvate injections. **(C)** Changes in precursor-product k_{PL} under different experimental conditions, including injection time intervals (0.5 h and 24 h) and administration orders (40mM followed by 80mM, and the reverse sequence.

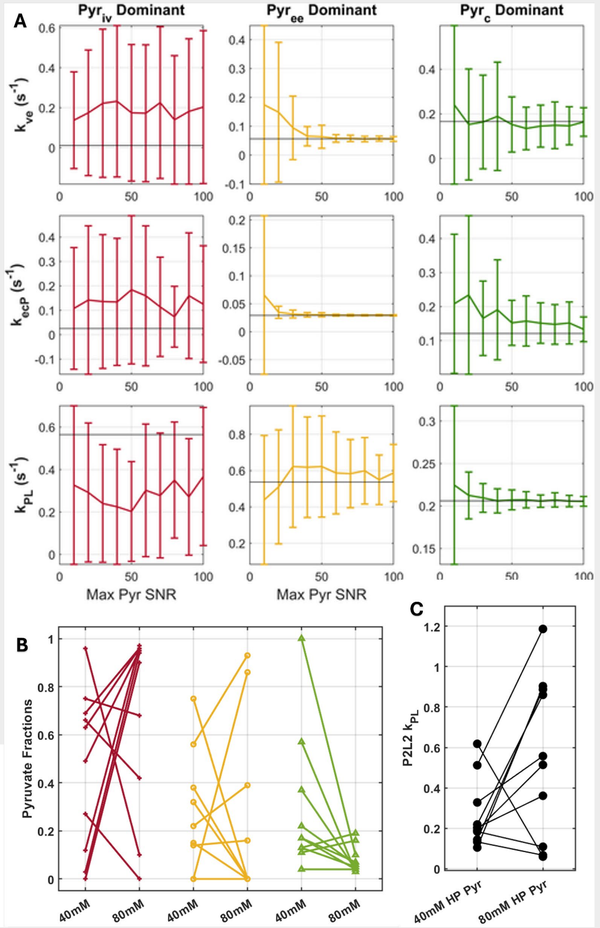

Figure 3. **(A)** Simulated accuracy and reproducibility of the fitted parameters in the simplified three-compartment PK model under varying pyruvate compartment distributions and signal noise ratio (SNR) levels[6]. **(B)** Pyruvate concentration fractions in the three compartments of ATC tumor tissue and corresponding changes between the 40mM and 80mM HP pyruvate injection. **(C)** Tumor tissue k_{PL} fitted using the two-compartment PK model. The accuracy and reproducibility of the fitted k_{PL} are supported by the predominance of intracellular pyruvate (green) shown in **B**.

ACKNOWLEDGMENT

This research was supported in part by funding from the National Cancer Institute of the National Institutes of Health (R01CA280980).

REFERENCES

1. O. Warburg, "On the Origin of Cancer Cells," *Science* 123, no. 3191 (1956): 309–314.
2. J. H. Ardenkjaer-Larsen, B. Fridlund, A. Gram, et al., "Increase in Signal-To-Noise Ratio of > 10,000 Times in Liquid-State NMR," *Proceedings of the National Academy of Sciences of the United States of America* 100, no. 18 (2003): 10158–10163.
3. P. E. Larson, R. Bok, A. B. Kerr, et al., "Investigation of Tumor Hyperpolarized [1-13C]-Pyruvate Dynamics Using Time-Resolved Multiband RF Excitation Echo-Planar MRSI," *Magnetic Resonance in Medicine* 63, no. 3 (2010): 582–591.
4. Bankson JA, Walker CM, et al., Kinetic Modeling and Constrained Reconstruction of Hyperpolarized [1-13C]-Pyruvate Offers Improved Metabolic Imaging of Tumors. Cancer Research. 2015;75(22):4708-17.
5. Michel KA, Ragavan M, Walker CM, Merritt ME, Lai SY, Bankson JA. Comparison of selective excitation and multi-echo chemical shift encoding for imaging of hyperpolarized [1-13C]pyruvate. Journal of Magnetic Resonance. 2021;325:106927.
6. R. T. Boyce, C. J. Harlan, Q. Wang, et al., " Physiological Interpretation of the Lactate to Pyruvate AUC Ratio for Hyperpolarized [1-13C]-Pyruvate Studies," Magnetic Resonance in Medicine 96, no. 1 (2026): 247–258,